

Structural properties of self-attracting walks

A. Ordemann,^{1,2} E. Tomer,² G. Berkolaiko,³ S. Havlin,² and A. Bunde¹

¹*Institut für Theoretische Physik III, Justus-Liebig-Universität Giessen, Heinrich-Buff-Ring 16, 35392 Giessen, Germany*

²*Minerva Center and Department of Physics, Bar-Ilan University, 52900 Ramat-Gan, Israel*

³*Department of Physics of Complex Systems, Weizmann Institute of Science, 76100 Rehovot, Israel*

(Received 12 February 2001; published 24 September 2001)

Self-attracting walks (SATW) with attractive interaction $u > 0$ display a swelling-collapse transition at a critical u_c for dimensions $d \geq 2$, analogous to the Θ transition of polymers. We are interested in the structure of the clusters generated by SATW below u_c (swollen walk), above u_c (collapsed walk), and at u_c , which can be characterized by the fractal dimensions of the clusters d_f and their interface d_I . Using scaling arguments and Monte Carlo simulations, we find that for $u < u_c$, the structures are in the universality class of clusters generated by simple random walks. For $u > u_c$, the clusters are compact, i.e., $d_f = d$ and $d_I = d - 1$. At u_c , the SATW is in a new universality class. The clusters are compact in both $d = 2$ and $d = 3$, but their interface is fractal: $d_I = 1.50 \pm 0.01$ and 2.73 ± 0.03 in $d = 2$ and $d = 3$, respectively. In $d = 1$, where the walk is collapsed for all u and no swelling-collapse transition exists, we derive analytical expressions for the average number of visited sites $\langle S \rangle$ and the mean time $\langle t \rangle$ to visit S sites.

DOI: 10.1103/PhysRevE.64.046117

PACS number(s): 68.35.Rh, 64.60.-i, 05.40.-a

I. INTRODUCTION

In previous years various models of random walks (RW) with memory or interaction have been studied [1–10] in order to account for distinct features of physical, chemical, and biological systems whose complexity goes beyond what can be obtained from the simple random walk picture. Perhaps the most extensive studied model is the self-avoiding walk (SAW), where the random walker is not permitted to step on already visited sites, simulating the behavior of linear polymers. Although all investigated RW models with memory are similar in the sense that they incorporate interactions between steps, they display quite distinct asymptotic properties. Therefore, they belong to universality classes that are usually different from RW or SAW, though they may cross over to either RW or SAW behavior in some limits. Common properties for describing the behavior of a walker are the exponents ν and k , characterizing the scaling with time t of the mean square end-to-end distance

$$\langle R^2(t) \rangle \sim t^{2\nu} \quad (1a)$$

and the average number of visited sites

$$\langle S(t) \rangle \sim t^k. \quad (1b)$$

For RW the exponents are $\nu = 1/2$ for all dimensions d , $k = 1/2$ for $d = 1$, and $k = 1$ for $d \geq 2$ [11]. For SAW, $k = 1$ for all d and $\nu \cong 3/(d+2)$ [12,13]. A comparative study [14] of some of these models [1,5,8,10] in one dimension has shown that the characteristic exponents depend crucially on the particular form of the interaction between the steps. Some of the important mechanisms are the range of the interaction, the presence of cumulative memory effects, and the global or local normalization conditions. Models with global and local normalization conditions are also referred to in the literature as static and dynamic models, respectively.

Recently, one of the dynamic models without cumulative memory effects, the self-attracting random walk (SATW)

[9], has been found to display, in contrast to all other models, a swelling-collapse transition at a critical attractive interaction u_c in $d \geq 2$ [15]. The characteristic exponents ν and k for SATW are in different universality classes for below u_c (swollen walk), at u_c , and above u_c (collapsed walk). Above and below criticality, ν and k have been determined analytically. At criticality, the exponents could only be studied numerically, and due to the finite-size effects close to a transition, there have remained open questions regarding the asymptotic behavior of SATW. A careful analysis of the simulation data and a scaling approach different from the one developed in Ref. [15] is found to be necessary for a comprehensive study of the structural properties of SATW, especially at critical $u = u_c$, which is the focus of this paper. To determine the fractal dimension of the cluster and the interface generated by the walker and to give more precise results for the characteristic exponents, we investigate the temporal development of the number of sites visited by the walker that have a certain amount of already visited next nearest neighbor sites. Identifying the sites belonging to the external and internal perimeter of the cluster in $d = 2$, the fractal dimensions of these structures are studied for attractions below, at, and above criticality.

The paper is organized as follows. In Sec. II several known RW models with interactions are summarized and their behavior is compared. The SATW model is briefly reviewed in Sec. III, presenting the analytical and numerical results for the mean square end-to-end distance and the average number of visited sites for varying strength of attractive interaction following [15], showing the evidence for the phase transition. In Sec. IV we investigate the structure of the cluster grown by the walker for different attractive interactions using a new approach consisting of scaling arguments and Monte Carlo simulations, which leads to more insight into the behavior of the system at criticality. We study the fractal dimensions of the cluster and its interface in $d = 2$ and $d = 3$. Closed form expressions for the average number of visited sites and the mean time to visit a certain

number of sites in $d=1$ are given in Sec. V. Finally, in Sec. VI we summarize our main results.

II. RW MODELS WITH INTERACTION

When a self-avoiding constraint like in the SAW model is added to the RW, the evolution of the walk becomes heavily dependent on the entire history of the walk, converting it into a non-Markovian system. A bridge between ordinary RW and non-Markovian walks can be constructed by associating energies $E_t(w)$ to all possible configurations w of a t -step random walk, defining an ensemble probability for a certain walk configuration as $P_t(w) = \exp[-\beta E_t(w)] / \sum_w \exp[-\beta E_t(w)]$, with $\beta = (k_B T)^{-1}$, where k_B is Boltzmann's constant and T is the absolute temperature. In the high-temperature limit all walks become equally likely, but at finite temperatures the ensemble probabilities of individual paths differ. If $E_t(w) < 0$ for walks with many visited sites, walks preferring to explore new terrain dominate the system, whereas if $E_t(w) > 0$ for walks with many visited sites, the system is governed by configurations of walks attracted to their own path. Models based on this concept are by definition in the class of static models, for a comprehensive overview see Ref. [11]. One straightforward way of modelling attractive and repulsive interaction between steps, known as the interacting walk [1], is to assign an energy $E_t(w) = g S_t(w)$ to a walk configuration, where $S_t(w)$ is the number of visited sites of a t -step RW configuration. For interaction parameter $g=0$ the simple random walk is recovered, while for $g < 0$ the walk becomes repulsive and the characteristic exponents are $\nu = k = 1$ in $d=1$ [2,3]. For $g > 0$ the walk is attractive and $k = 1/3$ and $2/3$, in $d=1$ and 2 , respectively, as well as $d/(d+2)$ in $d \geq 3$ [1,2,11].

In a more generalized static model including cumulative memory effects [4] the energy of a walk configuration is $E_t(w, \alpha) = g \sum_s n_t^\alpha(s)$ with $0 \leq \alpha \leq 2$, where $n_t(s)$ is the number of times a certain site s has been visited after t steps. For cumulative memory parameter $\alpha=0$ the previous model of Ref. [1] is recovered, and for $\alpha=2$ it is also known as the Domb-Joyce model [5,6], while for $g=0$ or $\alpha=1$ it reduces to simple random walks. The model is repulsive for $\alpha < 1$ and $g < 0$ or $\alpha > 1$ and $g > 0$; in the latter case Flory arguments give $\nu = (\alpha + 1)/(2 + \alpha d - d)$ independent of g for $d \leq d_c = 2\alpha/(\alpha - 1)$, where d_c is the critical dimension. For the attractive regime, results are only known in $d=1$, where for $\alpha < 1$ and $g > 0$ it exhibits continuous varying exponents depending on α with $\nu = k = (1 - \alpha)/(3 - \alpha)$, while for the other attractive branch $\alpha > 1$ and $g < 0$ it is always self-trapping as $\langle R \rangle$ and $\langle S \rangle$ saturate.

An approach analogous to the one above for the static models can be made for the less investigated dynamic models, where the local normalization is done by assigning a probability P_i to the walker to step to the next nearest neighbor site i during the evolution of the walk, with $P_i = \exp(g n_i^\alpha) / \sum_{i=1}^{2d} \exp(g n_i^\alpha)$, $\alpha > 0$. Here, n_i is the number of times the neighbor site i has already been visited in the previous t time steps [7]. For $g=0$ the simple random walk is recovered, while for $g < 0$ the walk is repulsive and the exponent ν is determined to be $\nu = (\alpha + 1)/(2 + \alpha d)$ for d

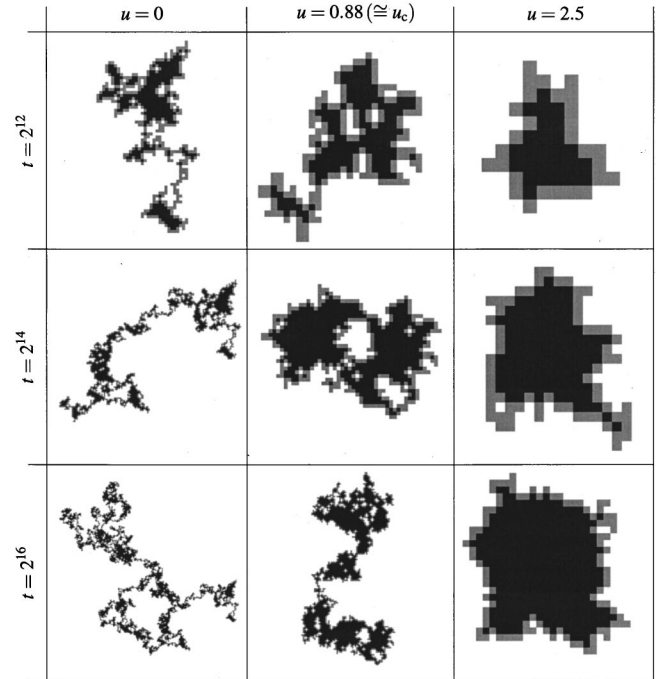


FIG. 1. Representative example of the structures grown by SATW after $t=2^{12}$, 2^{14} , and 2^{16} time steps for $u=0$, $u=0.88$ ($\cong u_c$), and $u=2.5$ in $d=2$. Gray sites form the interface, black sites are completely surrounded by already visited neighbor sites. The length scale is arbitrary chosen so that the clusters fill the size of the box. Note that for $u < u_c$, one can easily follow the growth process because of the distinctive structure of the cluster, while for $u = u_c$ it is difficult to follow, since the walker keeps coming back more often altering the structure. For $u > u_c$ it is not possible to do so as the grown clusters are compact.

$\leq d_c = 2$. For the attractive regime $g > 0$ it is known that in $d=1$ the walk is always self-trapping. A special case of this model is the true self-avoiding walk of Ref. [8] with $g < 0$ and $\alpha = 1$.

In surprising contrast to the results for all abovementioned models, where the characteristic exponents are always independent of the actual strength of the attraction or repulsion parameter g , are the results for the SATW model [9] focused on here. In this model a random walker jumps with probability $P_i = \exp(u n_i) / \sum_{i=1}^{2d} \exp(u n_i)$ [16] to a next nearest neighbor site i , with $n_i = 1$ for already visited sites and $n_i = 0$ for not visited sites. For $u > 0$, the walk is attracted to its own trajectory, so that SATW is an extension of Ref. [7] with attraction parameter $u = g > 0$ in the limit of no cumulative memory effect $\alpha \rightarrow 0$. Note that the results of Ref. [7] cannot be directly applied to the SATW model as they are based on the restriction $\alpha > 0$. Some representative examples of two-dimensional clusters grown by SATW for different values of u at three distinct times t of evolution are shown in Fig. 1. The exponents k and ν of SATW have been found to depend on u [9,17–19], although it was not clear for some time if ν and k decrease continuously with increasing u [18,19] or if a critical value u_c exists, below, at, and above which the exponents show different universal behavior [9,17]. Recently, it was found by exhaustive computer simulations with up to

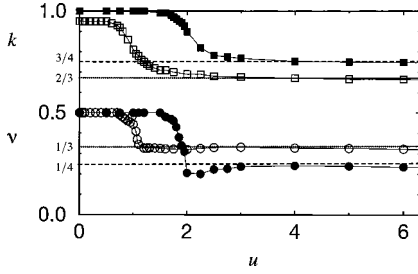


FIG. 2. The values of the exponents k (squares) and ν (circles) versus attraction u in $d=2$ (open symbols) and $d=3$ (filled symbols) for $t=10^8$, obtained by a least square fit of the slope of $\ln\langle R^2(t) \rangle$ and $\ln\langle S(t) \rangle$ versus $\ln t$ for large t , respectively. Note that for $u > u_c$ the values of k and ν approach the theoretical predictions of Eqs. (2), marked as dashed lines. The estimated values of u_c are $u_c = 0.88 \pm 0.05$ in $d=2$ and $u_c = 1.92 \pm 0.03$ in $d=3$.

$t = 5 \times 10^9$ time steps that there exists a swelling-collapse transition for SATW at a critical attraction u_c [15], analogous to the Θ transition in linear polymers at temperature $T = \Theta$ when an attraction term $\exp[-A/T]$, $A < 0$, is added to the self-avoiding constraint [12,13]. This phenomenon of a swelling-collapse transition can only occur because of a balance of the interaction energy and the configurational entropy of the SATW at criticality. When the energy is not of the order of the entropy as investigated in Ref. [7] for $\alpha > 0$, the walk collapses for any attraction $u = g > 0$.

III. SWELLING-COLLAPSE TRANSITION FOR SATW

In [15] it was shown that the characteristic exponents ν and k for SATW are in different universality classes for $u < u_c$, $u = u_c$, and $u > u_c$. Above u_c , the walk collapses for $d \geq 2$, and ν and k are given by

$$\nu = \frac{1}{d+1} \quad (2a)$$

and

$$k = \frac{d}{d+1}. \quad (2b)$$

Equations (2) follow (cf. [15]), since for sufficiently strong attraction $u > u_c$ the grown clusters are compact (see Fig. 1), so the average number of visited sites scales with the root mean square displacement $\langle R \rangle \equiv \langle R^2 \rangle^{1/2}$ as $\langle S \rangle \sim \langle R \rangle^d$. Comparing this to Eq. (1a) yields $k = \nu d$ for $u > u_c$. Also, the mean cluster growth rate is proportional to the ratio between the number of boundary sites and the total number of the cluster sites, $d\langle S \rangle / dt \sim \langle R \rangle^{d-1} / \langle R \rangle^d \sim t^{-\nu}$ [17,20]. Thus $\langle S \rangle \sim t^{-\nu+1}$. Combining these results with Eq. (1b), one obtains Eqs. (2). Below a critical interaction u_c , the walk swells and the exponents are as with no interaction [11], i.e., $\nu = 1/2$ and $k = 1$ for $d \geq 2$. The above analytic arguments are in good agreement with numerical simulations in $d=2$ and $d=3$ (see Fig. 2). At u_c , the exponents are numerically determined to be $\nu_c = 0.40 \pm 0.01$ and $k_c = 0.80 \pm 0.01$ for $d=2$ as well as $\nu_c = 0.32 \pm 0.01$ and $k_c = 0.91 \pm 0.03$ for $d=3$ [15]. Note that

for $d=1$ no swelling-collapse transition exists, as the walk is collapsed for all u , and Eqs. (2) reveal the known values $k = 1/2$ and $\nu = 1/2$ for random walk in $d=1$ [11,21] (see also Sec. V).

In the analogous static model of the interacting walk [1] with attractive interaction and no cumulative memory effects, a phase transition can not be observed due to the fact that the global normalization condition increases the weight of the interaction energy more than the local normalization condition, as already observed in Ref. [14] for $d=1$. This can also be seen from the asymptotic behavior of the characteristic exponent $k = d/(d+2)$ for the attractive interacting walk [1,11] in comparison to the ‘‘less collapsed’’ $k = d/(d+1)$, Eq. (2b), for the SATW discussed here. Therefore, a static interacting walk with the slightest attraction $u = g > 0$ has a qualitatively different behavior than the ordinary RW and is collapsed. Note that in both models k never becomes independent of the dimension, although it approaches unity from below in the large dimensionality limit.

Due to finite time effects at criticality it is not possible to determine the exponents ν_c and k_c more and more accurately by simply increasing the number t of time steps performed by the walker. As long as the attraction is slightly above or below criticality, as it is always the case in numerical simulations, the exponents will finally cross over to their expected values respectively above and below u_c after some time t . Introducing a crossover time t_ξ , below which the exponent ν is close to ν_c and above which ν approaches $1/2$ for $u < u_c$ and $1/(d+1)$ for $u > u_c$ (see Fig. 1 of Ref. [15]), the following scaling theory holds:

$$\langle R(t) \rangle \sim t^\nu f_\pm(t/t_\xi) \quad (3a)$$

with

$$t_\xi = |u - u_c|^{-\zeta}, \quad (3b)$$

where the plus sign refers to $u > u_c$, the minus sign to $u < u_c$, and the exponent ζ has to be determined numerically. As t_ξ is the only relevant time scale, the scaling functions bridge the short time and the long time regime. To match both regimes, it is required that $f_\pm(x) = \text{const}$ for $x \ll 1$ ($t \ll t_\xi$) and $f_+(x) \sim x^{1/(d+1) - \nu_c}$, $f_-(x) \sim x^{1/2 - \nu_c}$ for $x \gg 1$. An analogous scaling approach holds for $\langle S(t) \rangle$, and an excellent data collapse can be obtained for $\zeta = 7 \pm 1$ in $d=2$ and $\zeta = 5.0 \pm 0.5$ in $d=3$ (see Fig. 3 of Ref. [15]), confirming the numerical values for ν_c , k_c , and u_c determined from Fig. 2.

Since the mass of the cluster generated by the walker, consisting of all visited sites, scales as

$$\langle S \rangle \sim \langle R \rangle^{k/\nu}, \quad (4)$$

the ratio k/ν corresponds to the fractal dimension d_f of the cluster,

$$d_f = \frac{k}{\nu}. \quad (5)$$

In $d=2$ the clusters are compact for all u as $k/\nu = d_f = d$. In $d=3$ they are compact for $u > u_c$, while for $u < u_c$, the frac-

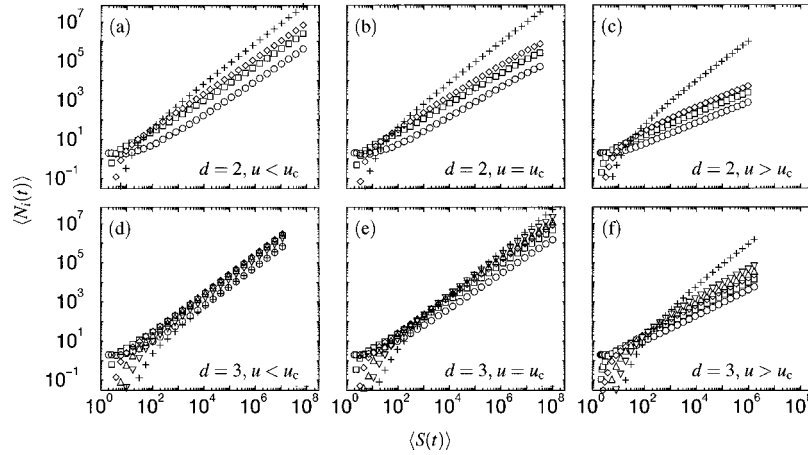


FIG. 3. The average number of cluster sites $\langle N_i(t) \rangle$ having i already visited nearest neighbor sites plotted versus the average number of all cluster sites $\langle S(t) \rangle$ up to $t=2 \times 10^9$ time steps (for $u < u_c$ in $d=2$ and $d=3$ only up to $t=10^9$ and $t=3 \times 10^7$, respectively) averaged over 100 configurations in $d=2$ for (a) $u=0.5 < u_c$, (b) $u=0.88 \cong u_c$, (c) $u=2.5 > u_c$, and in $d=3$ for (d) $u=1 < u_c$, (e) $u=1.92 \cong u_c$, and (f) $u=4 > u_c$. In $d=2$ the data for the different values of i are marked by $i=1$ (circles), $i=2$ (squares), $i=3$ (diamonds), and $i=4$ (pluses), whereas in $d=3$, $i=1$ (circles), $i=2$ (squares), $i=3$ (diamonds), $i=4$ (upward triangles), $i=5$ (downward triangles), and $i=6$ (pluses). Note that (d) clearly differs from (a), (b), (c), and (f). The values of the slopes a_i determined from the data are summarized in Table II.

tal dimension of clusters generated by simple random walks $d_f=2 < d$ is obtained. At the criticality, d_f was found numerically to be $d_f=2.84 \pm 0.25$, but the possibility that $d_f=d$ could not be ruled out in Ref. [15].

IV. THE CLUSTER AND ITS INTERFACE AT CRITICALITY

To clarify if the grown clusters in $d=3$ at $u=u_c$ are compact or fractal and to learn more about the structure of the SATW clusters and their interfaces at criticality, we consider the following: Denoting by $N_i(t)$ the number of cluster sites that have i of their $2d$ next nearest neighbor sites belonging to the cluster after t time steps, the number of all cluster sites $S(t)$ is the sum of all $N_i(t)$,

$$S(t) = N_1(t) + N_2(t) + \dots + N_{2d}(t). \quad (6)$$

The cluster growth rate is *equal* to the probability to be on the boundary of the cluster multiplied by the conditional probability to expand the cluster while being on its boundary. Suppose the walker is on a site that has i visited next nearest neighbor sites. As the probability to step to a next nearest neighbor site is $P \sim \exp(-un)$, with $n=1$ for already visited sites and $n=0$ for unvisited sites, the probability to jump to a visited neighbor site is proportional to $i \exp(-u)$, whereas the probability to jump to an unvisited neighbor site is proportional to $2d-i$. Thus the normalized probability \tilde{P}_i to expand, i.e., to jump to one of the $2d-i$ unvisited next nearest neighbor sites, is given by

$$\tilde{P}_i = \frac{2d-i}{i \exp(u) + 2d-i}. \quad (7)$$

Therefore, the average cluster growth rate is

$$\frac{d\langle S \rangle}{dt} = \tilde{P}_1 \frac{\langle N_1 \rangle}{\langle S \rangle} + \tilde{P}_2 \frac{\langle N_2 \rangle}{\langle S \rangle} + \dots + \tilde{P}_{2d-1} \frac{\langle N_{2d-1} \rangle}{\langle S \rangle}. \quad (8)$$

The situation $i=2d$ is special because $\tilde{P}_{2d}=0$ as the cluster cannot be expanded from a site where all surrounding sites already belong to the cluster. Assuming that the average number of cluster sites $\langle N_i \rangle$ that have i already visited nearest neighbor sites scales as

$$\langle N_i \rangle \sim \langle S \rangle^{a_i}$$

with

$$0 \leq a_i \leq 1, \quad (9)$$

there must be at least one i for which $a_i=1$ to ensure that Eq. (6) holds. In general, one can distinguish between two different cases: (i) there exists at least one $i < 2d$ for which $a_i=1$ (ii) only $a_{2d}=1$.

In case (i), the average cluster growth rate $d\langle S \rangle/dt$ is dominated by the $\langle N_i \rangle$ for which $a_i=1$, leading to $d\langle S \rangle/dt \sim \tilde{P}_i \langle N_i \rangle / \langle S \rangle = \tilde{P}_i \langle S \rangle^{a_i} / \langle S \rangle = \text{const}$. Therefore, in this case one gets $k=1$ as $\langle S \rangle \sim t$. In case (ii), when only $a_{2d}=1$, the cluster growth rate is dominated by the $\langle N_i \rangle$ for which $a_i = a_{\max} = \max\{a_1, a_2, \dots, a_{2d-1}\}$. This gives $d\langle S \rangle/dt \sim \langle S \rangle^{a_{\max}} / \langle S \rangle = \langle S \rangle^{a_{\max}-1}$, and hence

$$k = \frac{1}{2 - a_{\max}} \quad (10)$$

when compared to Eq. (1b). As shown below, the grown cluster is fractal for case (i) while for case (ii) it is compact.

The above considerations also enable us to determine numerically the exponent k in a way different from Ref. [15], and additionally to gain more insight into the grown structures, especially in the regime at $u=u_c$. Figure 3 shows that the assumption of Eq. (9) is clearly supported by numerical

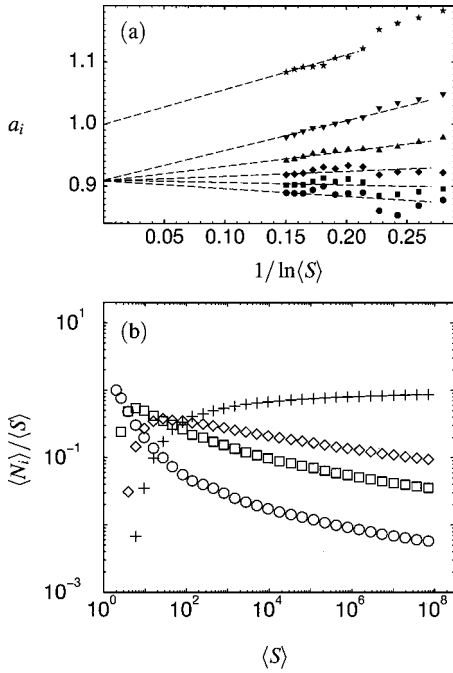


FIG. 4. (a) The successive slopes $a_i = d \ln \langle N_i \rangle / d \ln \langle S \rangle$ of the data from Fig. 3(e) plotted versus $1/\ln \langle S \rangle$. A linear extrapolation of the points to the limit $1/\ln \langle S \rangle \rightarrow 0$ yields our estimates $a_i = 0.91 \pm 0.01$ for $1 \leq i < 2d$ and $a_{2d} = 1.00 \pm 0.01$, clearly revealing that this regime belongs to case (ii). The data are marked as in Fig. 3(e). (b) The average number of cluster sites having i already visited nearest neighbors divided by the average number of all cluster sites $\langle N_i(t) \rangle / \langle S(t) \rangle$ versus $\langle S(t) \rangle$ of the data from Fig. 3(a). Note that the data for $i=4$ marked by pluses show a dominant behavior compared to the data for $i=1$ (circles), $i=2$ (squares), and $i=3$ (diamonds), implying that the regime $u < u_c$ in $d=2$ belongs to case (ii).

results. When plotting $\langle N_i \rangle$ versus $\langle S \rangle$, the decision as to which case (i) or (ii) a certain regime belongs becomes obvious from Fig. 3 for all regimes except for $u = u_c$ in $d=3$. For $u < u_c$ in $d=3$ we observe case (i) [see Fig. 3(d)], as $a_i = 1$ for all i . The other regimes belong to case (ii) [see Figs. 3(a)–3(c) and 3(f)] since only $a_{2d} = 1$. At $u = u_c$ in $d=3$ [Fig. 3(e)], a more detailed investigation of the results is necessary. By plotting the successive slopes $a_i = d \ln \langle N_i \rangle / d \ln \langle S \rangle$ of the data of Fig. 3(e) versus $1/\ln \langle S \rangle$ [Fig.

TABLE I. The exponents ν and k as well as the estimated values for the transition point u_c for SATW in $d=2$ and $d=3$.

		$u < u_c$	$u = u_c$	$u > u_c$
$d=2$	ν	1/2	0.40 ± 0.01	1/3
	k	1	0.80 ± 0.01	2/3
			$u_c = 0.88 \pm 0.05$	
$d=3$	ν	1/2	0.303 ± 0.005	1/4
	k	1	0.91 ± 0.01	3/4
			$u_c = 1.92 \pm 0.03$	

4(a)], it becomes obvious that only $a_{2d} = 1$. Thus this regime belongs to case (ii). Moreover, Fig. 4(a) indicates that all $a_1, a_2, \dots, a_{2d-1}$ asymptotically have the same value, so $a_{\max} = a_1 = a_2 = \dots = a_{2d-1}$. As this is also found for all other regimes, in the following we will denote $a_1 = a_i$ for all $1 \leq i \leq 2d-1$ in both cases (i) and (ii), in distinction to a_{2d} . The values of the exponents are summarized in Table II, confirming the previous results for the exponent k (see Table I) when following Eq. (10). At $u = u_c$ in $d=3$, k_c can be determined more precisely than in Ref. [15] to be $k_c = 0.91 \pm 0.01$. Note that another approach to confirm our numerical results for k is to plot $\langle N_i \rangle$ versus t in a double logarithmic plot. Denoting the resulting slopes as κ_i , we expect

$$\kappa_i = k a_i \quad (11)$$

as $\langle N_i \rangle \sim \langle S \rangle^{a_i} \sim t^{k a_i} \sim t^{\kappa_i}$ when combining Eqs. (1b) and (9). The numerical values determined for κ_i are summarized in Table II and are in excellent agreement with the values determined for a_i when comparing with Eq. (11).

When examining the distinction between cases (i) and (ii), it becomes clear that the structures grown by the walker in case (i) are fractal while the ones in case (ii) are compact. This can be explained by considering that in case (ii) the sites that do not belong to the interface dominate the growth process as $a_{2d} > a_1$, leading to a compact structure (i.e., $d_f = d$). In case (i) all sites have the same contribution to the growth of the structure due to $a_{2d} = a_1$ [22]. As we found that $u = u_c$ in $d=3$ belongs to case (ii) [see Fig. 4(a)], the structure must be compact and we can definitely conclude that in this regime d_f has to be $d_f = d = 3$, correcting the value 2.84

TABLE II. The exponents a_i and κ_i for $1 \leq i < 2d$ and $i = 2d$ for all three regimes $u < u_c$, $u = u_c$, and $u > u_c$ in $d=2$ and $d=3$ from numerical simulations. The errors are of the order of 1%. For $u < u_c$ in $d=2$, most probably due to logarithmic corrections [24], it is not possible to obtain the asymptotic value of the exponents in numerical simulations, therefore we give them in parentheses. Note that the results for a_i for the regimes $u < u_c$ and $u > u_c$ are supported by combining $k = 1/2$ and Eq. (10) as well as Eqs. (2b) and (10), respectively.

		$u < u_c$		$u = u_c$		$u > u_c$	
		a_i	κ_i	a_i	κ_i	a_i	κ_i
$d=2$	$1 \leq i < 2d$	0.95(1)	0.90(1)	0.75	0.60	0.50	0.33
	$i = 2d$	1	0.95(1)	1	0.80	1	0.67
$d=3$	$1 \leq i < 2d$	1	1	0.91	0.83	0.67	0.50
	$i = 2d$	1	1	1	0.91	1	0.75

TABLE III. The fractal dimension d_f of the cluster and $d_I = a_I d_f$ of the interface grown by SATW for all three regimes $u < u_c$, $u = u_c$, and $u > u_c$ in $d=2$ and $d=3$. Additionally in $d=2$ the fractal dimensions of the external perimeter d_{EP} and the internal perimeter d_{IP} are given. In $d=3$ it is particularly not clear whether the external or the internal perimeter dominates the interface at $u = u_c$. In case no error bars are given, the numerical results are supported by analytical considerations.

	$u < u_c$	$u = u_c$	$u > u_c$
d_f	2	2	2
d_I	2	1.50 ± 0.01	1
$d=2$	d_{EP}	$4/3$	1.25 ± 0.05
	d_{IP}	2	1.50 ± 0.01
$d=3$	d_f	2	3
	d_I	2	2.73 ± 0.03

± 0.25 obtained earlier [15]. The latter value was calculated by combining the numerical results for the exponents $k_c = 0.91 \pm 0.03$ and $\nu_c = 0.32 \pm 0.01$ following Eq. (5). From the new numerical result $k_c = 0.91 \pm 0.01$ and $\nu_c = k_c/d_f = k_c/d$, we obtain the more accurate estimate $\nu_c = 0.303 \pm 0.005$.

Next we focus on the interface of the grown cluster. The total interface can be divided into the external perimeter, which is usually the more interesting fraction as it constitutes the reaction front with the environment, and the internal perimeter, which is the boundary of the inner holes of the cluster [23]. First we investigate the total interface. Its mass I is equal to $N_1 + N_2 + \dots + N_{2d-1}$ and therefore scales as

$$\langle I \rangle \sim \langle S \rangle^{a_I}. \quad (12)$$

Combining Eqs. (4) and (5) with Eq. (12) yields $\langle I \rangle \sim \langle R \rangle^{a_I d_f}$. Hence the fractal dimension d_I of the interface is simply

$$d_I = a_I d_f. \quad (13)$$

The values for d_I according to Eq. (13) are given in Table III. For $u < u_c$, we recover the values for normal random walks [11,24], $d_I = 2$ in $d=2$ and 3. As the fractal dimension of the external perimeter of a random walk is $d_{EP} = 4/3 < d_I$ in $d=2$ [11], this suggests that the internal perimeter is dominating the interface for $u < u_c$. In contrast, in $d=3$ the external perimeter governs the interface, $d_{EP} = 2 = d_I$ [11], as three-dimensional holes are less likely than two-dimensional ones due to geometrical constraints. For $u > u_c$, we find $d_I = d - 1$, clearly confirming the assumption that the structure of this regime is collapsed (see Fig. 1). It forms a compact disk a compact sphere, respectively, with a rather smooth surface and holes only in the surface layer. The clusters are similar to the clusters grown in the Eden model [25], where each unvisited next nearest neighbor site of the cluster has the *same* probability to be occupied at the given time step. It remains an open question whether these clusters are in the same universality class as one has to check if the surface for $u > u_c$ resembles the self-affine surface of the Eden cluster. At u

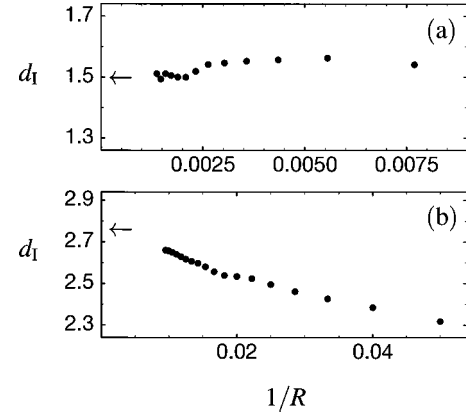


FIG. 5. The successive slopes $d_I = d \ln(I(R))/d \ln R$ of the mean mass $\langle I(R) \rangle$ of the interface inside a disk and a sphere of radius R plotted versus $1/R$ for $u = u_c$ at $t = 3 \times 10^8$ and $t = 3 \times 10^7$ time steps, respectively, averaged over 1000 configurations. A linear extrapolation of the points to the limit $1/R \rightarrow 0$ yields our estimates (a) $d_I = 1.50 \pm 0.02$ in $d=2$ and (b) $d_I = 2.72 \pm 0.04$ in $d=3$, confirming the results summarized in Table III, which are marked by an arrow.

$= u_c$, the structure of the interface is fractal in both $d=2$ and 3 with the values of $d_I = 1.50 \pm 0.01$ and $d_I = 2.73 \pm 0.03$, respectively. The rather surprising result for d_I in $d=3$ can be understood when considering that the structure of the interface at $u = u_c$ is more compact than for $u < u_c$ but the cluster is not collapsed as for $u > u_c$.

A straightforward way to confirm the above numerical results for d_I is to determine the fractal dimension of the interface by measuring it directly on the grown clusters instead of calculating it dynamically during the growth process. Using the sandbox method [26], the outcome supports the results stated above, although they are less precise due to the fact that the information about the growth process is lost. For the results of d_I at criticality in $d=2$ and $d=3$, see Fig. 5, showing a good agreement with the values summarized in Table III and clearly excluding the value of $d_f = 2.84$ determined in Ref. [15] for $d=3$, which would lead to $d_I = 2.58$ when following Eq. (13).

A further interesting question is which perimeter, external or internal, is dominating the interface of the clusters at criticality, and what is the actual value of the nondominating perimeter. Using the approach of Ref. [27] to identify the sites N_{EP} belonging to the external perimeter of a cluster in $d=2$, and identifying the internal perimeter sites N_{IP} as the interface sites not belonging to N_{EP} , we expect the average number of external perimeter sites $\langle N_{EP} \rangle$ to scale as

$$\langle N_{EP} \rangle \sim \langle S \rangle^{a_{EP}} \quad (14a)$$

and the average number of internal perimeter sites $\langle N_{IP} \rangle$ to scale as

$$\langle N_{IP} \rangle \sim \langle S \rangle^{a_{IP}}. \quad (14b)$$

Following the reasoning leading to Eq. (13) yields

$$d_{EP} = a_{EP} d_f \quad (15a)$$

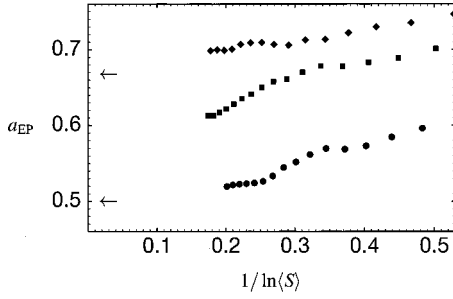


FIG. 6. The successive slopes $a_{EP} = d \ln \langle N_{EP} \rangle / d \ln \langle S \rangle$ plotted versus $1/\ln \langle S \rangle$ averaged over 500 configurations for $u = 0.5 < u_c$ (diamonds) up to $t = 10^7$ time steps, for $u = u_c$ (squares) up to $t = 10^8$ time steps, and for $u = 2.5 > u_c$ (circles) up to $t = 2 \times 10^9$ time steps in $d = 2$. A linear extrapolation of the points to the limit $1/\ln \langle S \rangle \rightarrow 0$ yields our estimates $a_{EP} = 0.68 \pm 0.02$ and 0.50 ± 0.02 for below and above u_c , respectively, confirming the results summarized in Table III, which are marked by an arrow. At u_c , a_{EP} is clearly smaller than for below u_c .

and

$$d_{IP} = a_{IP} d_I. \quad (15b)$$

The results for a_{EP} (see Fig. 6) recover the expected behavior of $d_{EP} = 4/3$ for $u < u_c$ and indicate that at criticality d_{EP} is clearly smaller than for below u_c , although it is difficult to determine the precise value of d_{EP} from this plot. Thus, at u_c the interface is dominated by the internal perimeter as $d_{EP} < d_I$. This is confirmed by the results for a_{IP} at criticality, where the expected value of $d_{IP} = d_I = 1.5$ is recovered, although with unsatisfactory precision [28]. Using the sandbox method [26] to measure the fractal dimension of the perimeter directly, the results support $d_{IP} = 1.5$ more precisely and we find $d_{EP} = 1.25 \pm 0.05$ for $u = u_c$ [see Fig. 7(a)]. The fact

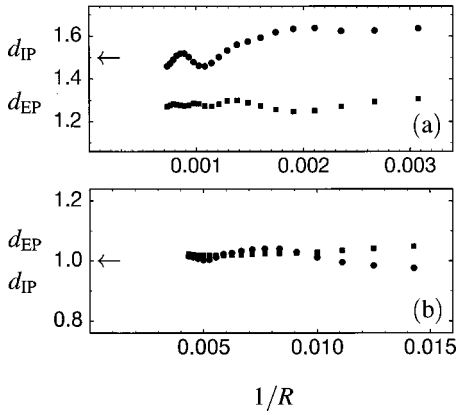


FIG. 7. The successive slopes for $d_{EP} = d \ln \langle N_{EP} \rangle / d \ln R$ and $d_{IP} = d \ln \langle N_{IP} \rangle / d \ln R$ of the mean mass $\langle N_{EP} \rangle$ and $\langle N_{IP} \rangle$ of the external and internal perimeter, respectively, plotted versus $1/R$ for (a) $u = u_c$ at $t = 10^8$ time steps and (b) $u = 2.5 > u_c$ at $t = 2 \times 10^9$ time steps averaged over 500 configurations in $d = 2$. A linear extrapolation of the points to the limit $1/R \rightarrow 0$ yields our estimates (a) $d_{IP} = 1.48 \pm 0.05$ (circles) and (b) $d_{EP} = 1.02 \pm 0.03$ (squares) and $d_{IP} = 1.01 \pm 0.03$ (circles), confirming the results summarized in Table III, which are marked by an arrow. At u_c , d_{EP} (squares) is determined to be $d_{EP} = 1.25 \pm 0.05$.

that d_{EP} for $u < u_c$ is definitely smaller than d_{EP} at $u = u_c$ reinforces that at criticality the SATW model is in a new universality class. For $u > u_c$ one might expect that the interface is dominated by the external perimeter due to the collapsed structure of the cluster. However, we find that the internal and the external perimeter contribute equally to the interface, $d_{IP} = d_{EP} = 1 = d_I$ [see Fig. 7(b)].

In $d = 3$, the fractal dimension of the external perimeter is $d_{EP} = 2 = d_I$ for $u < u_c$, supposing that d_{EP} follows the random walk result [11] like all other characteristic values determined for the SATW in this regime. Unfortunately it is not possible to determine d_{EP} or d_{IP} in $d = 3$ numerically using the algorithm of [27] to check which one, the external or the internal perimeter, governs the behavior at u_c , and to decide whether the external perimeter dominates the interface for $u > u_c$ i.e., $d_{EP} = d_I > d_{IP}$ or if $d_{EP} = d_I = d_{IP}$ in this regime. The values for d_{EP} and d_{IP} according to the above considerations are given in Table III.

V. SATW IN ONE DIMENSION

As we mentioned above, in $d = 1$ there is no swelling-collapse transition as the walk is collapsed for all u . The exponents k and ν are $k = 1/2$ and $\nu = 1/2$ [11,21] in accordance with Eqs. (2). Following the considerations leading to Eq. (10), the probability of the walker to be on the boundary of a SATW cluster is $\langle N_1 \rangle / \langle S \rangle = 2 / \langle S \rangle$, therefore SATW in $d = 1$ belongs to case (ii), since $a_1 = a_{\max} = a_I = 0$ and $a_{2d} = 1$. Thus, $k = 1 / (2 - a_{\max}) = 1/2$ as expected from analytical results [21]. Note that, based on Eq. (8), one can derive (although not rigorously) a closed form expression for $\langle S(t) \rangle$ in $d = 1$, extending the results of Ref. [21]. Since in $d = 1$ the conditional probability to expand the cluster while being on a perimeter site is $\tilde{P}_1 = 1 / [\exp(u) + 1]$ [cf. Eq. (7)] and $N_1 = 2$, we obtain

$$\frac{d \langle S(t) \rangle}{dt} = \frac{1}{\exp(u) + 1} \frac{2}{\langle S(t) \rangle}, \quad (16)$$

yielding

$$\langle S(t) \rangle = \left(\frac{2t}{\exp(u) + 1} \right)^{1/2}. \quad (17)$$

This result is strongly supported by numerical simulations (see Fig. 8).

In $d = 1$ it is also possible to solve the inverse problem of deriving the average time $\langle t(S) \rangle$ to visit a fixed number of visited sites S ,

$$\langle t(S) \rangle = S - 1 + \frac{(S-2)(S-1)(1-\tilde{P}_1)}{2\tilde{P}_1}. \quad (18)$$

For asymptotically large S , Eq. (18) yields $\langle t(S) \rangle \sim S^2$, recovering the expected scaling with $k = 1/2$. To derive Eq. (18) we use the standard approach to RW in $d = 1$ (see, for instance, Ref. [29]): The number of sites S visited by a

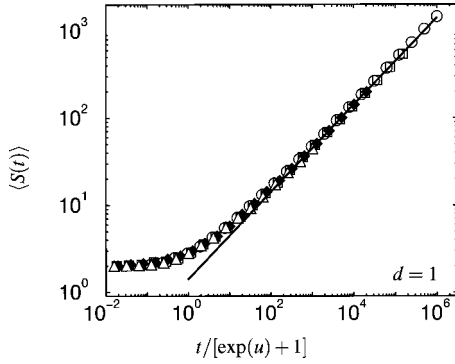


FIG. 8. The average number of visited sites $\langle S(t) \rangle$ in $d=1$ for different values of u , $u=2$ (circles), $u=4$ (squares), $u=6$ (diamonds), and $u=9$ (triangles), plotted versus time t scaled by $[1 + \exp(u)]^{-1}$ shows a good data collapse in agreement with Eq. (17) (solid line). The plateau for small t corresponds to the average time [equal to $1 + \exp(u)$] needed for the walker to escape the initial cluster of size 2.

walker in $d=1$ is equal to the span of the random walk. The time $t(S)$ passed before the span reaches S can be represented as the sum

$$t(S) = \sum_{i=2}^S \chi_i \quad (19)$$

with $\chi_i = t(i) - t(i-1)$ being the time spent before the span increases from $i-1$ to i , given that the walker is initially at the boundary. Thus, the mean time $\langle t(S) \rangle$ to visit S sites can be calculated as

$$\langle t(S) \rangle = \sum_{i=2}^S \langle \chi_i \rangle \quad (20)$$

with $t(1)=0$ and $t(2)=1$. Let us consider the nature of the variable χ_i in some detail. When at the boundary, the walker increases the span with the probability of success \bar{P}_1 . With probability $1 - \bar{P}_1$ the walker stays inside the cluster and undertakes an excursion until it hits the boundary again, which presents him with another opportunity to increase the span. We introduce the random variable μ , which is the number of unsuccessful attempts before the span is increased. In other words, μ is the number of excursions into the cluster, and with probability $\bar{P}_1(1 - \bar{P}_1)^m$, $m \geq 0$, μ is equal to m . Now we can decompose the χ_i as

$$\chi_i = 1 + \sum_{j=1}^{\mu} (\tau_j + 1), \quad (21)$$

where τ_j is the length of the j th excursion, and 1 is added to account for the jump from the boundary into the cluster before the excursion started. The random variable τ_j can be viewed as the time a random walker, starting at site 1 with the boundaries at 0 and $i-2$, needs to reach a boundary. Its mean is known to be $\langle \tau_j \rangle = i-3$ [29]. The mean of χ_i is just the average number of excursions multiplied by the average

length of one excursion. More rigorously, we express $\langle \chi_i \rangle$ in terms of conditional averages as follows:

$$\begin{aligned} \langle \chi_i \rangle &= \left\langle 1 + \sum_{j=1}^{\mu} (\tau_j + 1) \right\rangle \\ &= 1 + \sum_{m=1}^{\infty} \left\langle \sum_{j=1}^{\mu} (\tau_j + 1) \middle| \mu = m \right\rangle P(\mu = m). \end{aligned} \quad (22)$$

The variables τ_j are independent identically distributed random variables, therefore

$$\begin{aligned} \langle \chi_i \rangle &= 1 + \sum_{m=1}^{\infty} m \langle \tau_j + 1 \rangle P(\mu = m) \\ &= 1 + (i-2) \sum_{m=1}^{\infty} m \bar{P}_1 (1 - \bar{P}_1)^m \\ &= 1 + \frac{(i-2)(1 - \bar{P}_1)}{\bar{P}_1}. \end{aligned} \quad (23)$$

By combining Eqs. (20) and (23) one obtains Eq. (18).

VI. CONCLUDING REMARKS

In contrast to all other known random walk models with interaction, the SATW model exhibits a swelling-collapse transition at a critical attraction u_c in $d \geq 2$. The transition is similar to the swelling-collapse transition observed at the “ Θ point,” $T = \Theta$ of SAW with an attraction term $\exp[-A/T]$, $A < 0$ [12,13]. It can only arise because the attractive interaction energy is of the same order as the configurational entropy in $d \geq 2$. Below u_c the entropy dominates and the walk is in the universality class of simple RW, above u_c the energy governs the behavior and the walk collapses. At u_c , both contributions balance each other, leading to a new universality class. In $d=1$, due to a small number of possible configurations caused by the geometrical constraints, the walk is always collapsed, even without interaction $u=0$.

Analyzing the structure of the cluster grown by SATW in detail, we determined the fractal dimension of the cluster and its interface. In $d=2$, the cluster is always compact while the interface has a fractal dimension $d_I=2$ and 1.50 ± 0.01 below and at u_c , respectively, dominated by the internal perimeter. Above u_c , we found $d_I = d_{IP} = d_{EP} = 1$. The fractal dimension of the external perimeter at u_c , $d_{EP} = 1.25 \pm 0.05$, is smaller than below u_c , $d_{EP} = 4/3$, demonstrating once more the universality class at criticality. In $d=3$ the cluster is compact for $u \geq u_c$, while for $u < u_c$ the fractal dimension is $d_f=2$. Probably the most unexpected result is that in $d=3$ the

interface has a fractal dimension $d_I=2$ above and below u_c , whereas at criticality it increases to $d_I=2.73\pm 0.03$. This appealing structure at u_c is of interest on its own regarding that many challenging problems in physics, chemistry, and biology are associated with growth patterns in clusters and solidification fronts. The results for the fractal dimensions of the perimeters could also be helpful when investigating the structure of the cluster grown by SAW at the corresponding Θ transition, where sufficiently large clusters are difficult to

simulate because of the attrition of the walkers when stepping into their own dead ends.

ACKNOWLEDGMENTS

Financial support from the German-Israeli Foundation (GIF), the Minerva Center for Mesoscopics, Fractals, and Neural Networks, and the Deutsche Forschungsgemeinschaft is gratefully acknowledged.

-
- [1] H.E. Stanley, K. Kang, S. Redner, and R.L. Blumberg, *Phys. Rev. Lett.* **51**, 1223 (1983); **54**, 1209 (1985).
- [2] S. Redner and K. Kang, *Phys. Rev. Lett.* **51**, 1729 (1983).
- [3] D.Y.C. Chan and B.D. Hughes, *J. Phys. A* **17**, L121 (1984).
- [4] P.M. Duxbury and S.L.A. de Queiroz, *J. Phys. A* **18**, 661 (1985).
- [5] C. Domb and G.S. Joyce, *J. Phys. C* **5**, 956 (1972).
- [6] C. Domb, *J. Stat. Phys.* **30**, 425 (1983).
- [7] H.C. Oettinger, *J. Phys. A* **18**, L363 (1985).
- [8] D.J. Amit, G. Parisi, and L. Peliti, *Phys. Rev. B* **27**, 1635 (1983).
- [9] V.B. Sapozhnikov, *J. Phys. A* **27**, L151 (1994).
- [10] A. Malakis, *J. Phys. A* **8**, 1885 (1975); **9**, 1283 (1976).
- [11] B.D. Hughes, *Random Walks and Random Environments* (Clarendon Press, Oxford, 1995).
- [12] P.-G. de Gennes, *Scaling Concepts in Polymer Physics* (Cornell University Press, Ithaca, New York, 1979).
- [13] K. Barat and B.K. Chakrabarti, *Phys. Rep.* **28**, 377 (1995).
- [14] P.M. Duxbury, S.L.A. de Queiroz, and R.B. Stinchcombe, *J. Phys. A* **17**, 2113 (1984).
- [15] A. Ordemann, G. Berkolaiko, S. Havlin, and A. Bunde, *Phys. Rev. E* **61**, R1005 (2000).
- [16] Note that in the original definition by Sapozhnikov $P_i = \exp(-un_i)/\sum_{i=1}^{2d} \exp(-un_i)$ with $u < 0$ [17], for convenience we use $P_i = \exp(+un_i)/\sum_{i=1}^{2d} \exp(+un_i)$ with $u > 0$.
- [17] V.B. Sapozhnikov, *J. Phys. A* **31**, 3935 (1998).
- [18] F.D.A. Aaroro Reis, *J. Phys. A* **28**, 3851 (1995).
- [19] J.W. Lee, *J. Phys. A* **31**, 3929 (1998).
- [20] R. Rammal and J. Toulouse, *J. Phys. (France) Lett.* **44**, L13 (1983).
- [21] M.A. Prasad, D.P. Bhatia, and D. Arora, *J. Phys. A* **29**, 3037 (1996).
- [22] Although asymptotically $a=a_{2d}=1$ in $d=2$ for $u < u_c$ (see Table II), this regime belongs to case (ii) as a_{2d} is dominating the growth as can be seen in Fig. 4(b) where $\langle N_i \rangle / \langle S \rangle$ is plotted versus $\langle S \rangle$, most probably due to logarithmic corrections of the exponents [24].
- [23] A union U of two fractal sets A and B with fractal dimension d_A and d_B , respectively, has a fractal dimension $d_U = \max\{d_A, d_B\}$ [25]. Here, the total interface is a union of the external and the internal perimeters.
- [24] G.H. Weiss, and J.R. Rubin, *J. Chem. Phys.* **52**, 363 (1983).
- [25] T. Vicsek, *Fractal Growth Phenomena*, 2nd ed. (World Scientific, Singapore, 1992).
- [26] *Fractals and Disordered Systems*, 2nd ed., edited by A. Bunde and S. Havlin (Springer, Heidelberg, 1996).
- [27] J.-F. Gouyet, H. Harder, and A. Bunde, *J. Phys. A* **20**, 1795 (1987).
- [28] The reason is insufficient data, since the running time for one walk configuration is considerably increased by the implementation of the algorithm for the determination of the external perimeter at several times t during the growth of the cluster.
- [29] A.N. Shiriaev, *Probability* (Springer, New York, 1996).